Aggregation of Spin Labeled Trichogin GA IV Dimers: Distance Distribution between Spin Labels in Frozen Solutions by PELDOR Data

A. D. Milov,[†] Yu. D. Tsvetkov,*[,†] F. Formaggio,[‡] S. Oancea,[‡] C. Toniolo,[‡] and J. Raap[§]

Institute of Chemical Kinetics and Combustion, Novosibirsk, 630090 Russian Federation, Institute of Biomolecular Chemistry, CNR, Department of Organic Chemistry, University of Padova, 35131 Padova, Italy, and Leiden Institute of Chemistry, Gorlaeus Laboratories, Leiden University, 2300 RA Leiden, The Netherlands

Received: April 20, 2003; In Final Form: September 30, 2003

Pulsed electron−electron double-resonance (PELDOR) and CW-ESR spectroscopies were used to study the dipole−dipole interaction of spin labels in frozen glassy solutions of mono- and double-labeled analogues of the 22-residue, the head-to-tail covalent dimer of the peptaibol antibiotic trichogin GA IV. The [TOAC-1] and [TOAC-1,19] dimers were studied in methanol and in a chloroform−toluene mixture. It was shown these dimer molecules do not form aggregates in methanol. However, in chloroform−toluene, the PELDOR signal of the mono-labeled dimer shows oscillations, due to the dipole−dipole interaction of the nitroxide spin labels. From the signal decay, the number of molecules per aggregate was estimated to be ∼2−3, depending on the concentration used. The contributions of inter- and intra-aggregate interactions of spin labels to the PELDOR signal decay were separated. The distance distribution functions of the intra-aggregate interactions range from 3.0 to 4.5 nm. The maxima are observed at 3.4 nm. From the PELDOR data, we obtained the functions of distance distributions of labels for the monomeric double-labeled peptide in methanol as well as for the same peptide isolated within aggregates of nonlabeled peptide molecules in chloroform−toluene. In the latter case, the distribution function is the most narrow with a maximum at a distance between the nitroxide spin labels of 2.8 nm, which is in agreeement with the theoretical distance between labels at corresponding residue positions of an α-helical structure.

Introduction

Recently, the method of spin labeling in combination with pulsed electron−electron double-resonance (PELDOR) and continuous wave (CW) ESR has been applied to investigate the structure of spin-labeled analogues of the peptaibol antibiotics trichogin GA IV and zervamicin.[1−8] Interest to the study of these peptides is caused by their specific ability to modify the membrane permeability.[9,10] In contrast to the 20-residue alamethicin and the shorter 16-residue zervamicin,[11] the 11-residue trichogin GA IV is clearly too short to overspan the phospholipid bilayer. It has been previously suggested that trichogin might act as a channel former, after either head-to-tail or head-to-head dimerization processes occur.[12] The possibility of a noncovalent head to tail association of trichogin molecules was earlier demonstrated in the crystal packing of hydrogen bonded trichogin helices.[13]

Recently, the formation of aggregates of trichogin GA IV has been detected by the PELDOR spectroscopy technique. The self-assembling properties have been investigated in both polar and apolar solvents to mimic the two different local membrane environments, i.e., the polar headgroup−water interface and the apolar core of the phospholipid double layer. The method applied to the mono-labeled analogues of trichogin GA IV and zervamicin has shown that frozen solutions of weakly polar solvents contain aggregates of the molecules.[3−5,8] However, in polar solution, the amphipathic molecules remain in the monomeric (nonaggregated) state.[5] It has also been found that peptide aggregates are present in apolar liquid solutions.[6,7] Analysis of the experimental data has indicated that the observed aggregates contain about four peptide molecules.[3−5] Some of us have shown[9,14] that the introduction of spin labels has no effect on the biophysical properties, but it favors the determination of the 3D structure of these molecules by analyzing the interactions between them.

In analogy with previous papers, in this work, we used the simplest version of the PELDOR technique, based on a two-pulse electron spin−echo at the resonance frequency ν_A with a pumping pulse added at another frequency (ν_B) to turn over a part of spins that do not participate in spin−echo formation. After the first mw-pulse, a pumping pulse is supplied at time T. This pulse changes the sign of the dipole−dipole interaction between the spins forming the spin−echo (spins A) and the spins excited by the pumping pulse (spins B). As a result, the spin−echo signal amplitude begins to depend on both the position of the pumping pulse, at T, and the probability p_b of spin B flips induced by the pumping pulse. The analysis of the dependence of the PELDOR signal on T and p_b provides information on the magnitude of dipole−dipole interactions between spin labels and on the number of spin labels in the aggregates.[17]

In this work, the PELDOR technique is exploited to examine spin labeled analogues of the head-to-tail, covalently bound trichogin dimers DT0, DT1, and DT2 in comparison with the previously studied, monomeric trichogin (MT0) analogues MT1 and MT2. The amino acid sequences of these peptides are as follows:

* To whom correspondence should be addressed. Prof. Yu. D. Tsvetkov, Institute of Chemical Kinetics and Combustion, Institutskaja str. 3, Novosibirsk, 630090 Russia. E-mail: tsvetkov@ns.kinetics.nsc.ru.
[†] Institute of Chemical Kinetics and Combustion.
[‡] University of Padova.
[§] Leiden University.

10.1021/jp035057x CCC: $25.00
Published on Web 11/15/2003

Oct-Aib-G−L-Aib-G−G-L-Aib-G−I-Lol *trichogin GA IV* (MT0)

Oct-TOAC-G−L-Aib-G−G-L-Aib-G−I-L-OMe (MT1)

Oct-TOAC-G−L-Aib-G−G-L-TOAC-G−I-L-OMe (MT2)

Ac-Aib-G−L-Aib-G−G-L-Aib-G−I-L-Aib-G−L-Aib-G−G-L-Aib-G−I-L-OMe (DT0)

Ac-TOAC-G−L-Aib-G−G-L-Aib-G−I-L-Aib-G−L-Aib-G−G-L-Aib-G−I-L-OMe (DT1)

Ac-TOAC-G−L-Aib-G−G-L-Aib-G−I-L-Aib-G−L-Aib-G−G-L-TOAC-G−I-L-OMe (DT2)

where Aib is α-aminoisobutyric acid, TOAC is 2,2,6,6,-tetramethylpiperidine-1-oxyl-4-amino-4-carboxylic acid, Ac is acetyl, Lol is leucinol, and L-OMe is leucine methyl ester. The spin labeled peptides DT1 and DT2, as compared with the prototypical peptide dimer DT0, are characterized by the nitroxyl spin labeled α-amino acid TOAC.[15,16] DT1 is labeled at position 1, whereas in DT2, TOAC replaces the two Aib residues at positions 1 and 19. As both TOAC and Aib are C^{α}-tetrasubstituted α-amino acids, the overall 3D-structure of the peptide dimers is not expected to be substantially modified by the Aib → TOAC replacements.[14,16] The chemical formulas of Aib and TOAC are shown below.

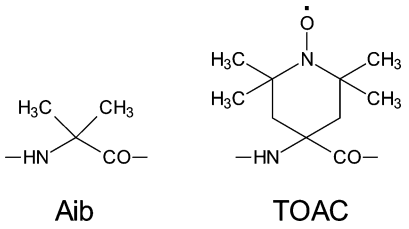

We investigated the inter- and intramolecular interactions of spin labels for frozen solutions of the DT1 and DT2 peptides in a chloroform−toluene mixture and in methanol (MeOH) with the aim at elucidating aggregate formation in solvents of different polarities. We assumed that the aggregates are preserved when the solutions are quickly frozen to liquid-nitrogen temperature as already observed for aggregates of trichogin GA IV.[6] A method is proposed to determine the function of distance distribution between spin labels from the PELDOR data, which allows us to obtain information about the structural features of the peptide molecules in the monomeric state and in the aggregates.

Experimental Section

Peptide Synthesis and Characterization. The head-to-tail dimers of trichogin GA IV (DT0, DT1, and DT2) were synthesized in solution by the fragment condensation technique. For each dimer, two appropriate 11-residue segments were coupled head-to-tail by exploiting the highly efficient EDC/HOAt[18] [EDC, 1-(3-dimethylaminopropyl)-3-ethylcarbodiimide; HOAt, 1-hydroxy-7-aza-1,2,3-benzotriazole] condensation method. In all cases, a final reverse-phase HPLC purification step was required. Details of the syntheses and analytical data for DT0, DT1, and DT2 are available as Supporting Information.

ESR. The ESR spectra of the spin-labeled peptide solutions frozen to 77 K were obtained in an ESP-380 Bruker spectrometer at a modulation frequency of 100 kHz and a modulation amplitude of 0.05 mT in the absence of CW ESR spectrum saturation. PELDOR studies were carried out using the home-made PELDOR spectrometer.[17] The duration of the first and second pulses forming the spin−echo signal were 50 and 80 ns, respectively. The duration of the pumping pulse was about 40 ns. The position of the pumping pulse corresponded to the maximum amplitude in the ESR spectrum. The frequency difference $\nu_A - \nu_B$ was 65 MHz. The value of p_b was determined experimentally from the time T dependence of the PELDOR signal for frozen glassy solutions of the double-labeled peptide DT2 in MeOH.[3−5] The value of p_b, under the above given experimental conditions, was determined to be 0.19.

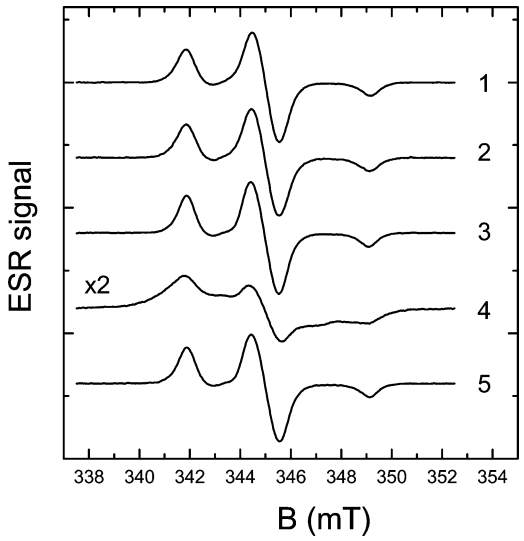

Figure 1. ESR spectra of the peptides studied in glassy solutions at 77 K: (1) DT1 in MeOH; (2) DT2 in MeOH; (3) DT1 in the chloroform−toluene (7:3) mixture; (4) DT2 in the chloroform−toluene (7:3) mixture; (5) DT2/DT0 (1:10) in the chloroform−toluene (7:3) mixture.

For the ESR and PELDOR studies, glassy ampules of 0.5 cm containing about 0.08 mL of the sample solution were used. As an apolar solvent, we exploited a chloroform−toluene mixture in the 7:3 ratio by volume. After freezing at 77 K, this mixture took the form of a transparent glass. As a polar solvent, we exploited methanol containing about 1% of water. The samples were prepared using spectroscopic grade methanol, chloroform, and toluene without repurification. Peptide concentration varied from 1.5×10^{-4} to 6×10^{-3} M. The samples were placed in a finger of the Dewar flask cooled with liquid nitrogen and located in the spectrometer resonator.

Theoretical structures of dimers of different conformations were calculated as previously described.[5]

Results and Discussion

CW-ESR Spectra. The CW-ESR spectra of the spin labeled peptides DT1 and DT2 in frozen glassy MeOH and in the frozen glassy chloroform−toluene (7:3) mixture at 77 K are shown in Figure 1.

Spectra 1 and 2 belong to peptides DT1 and DT2 in MeOH, whereas spectra 3 and 4 belong to the same peptides in the chloroform−toluene (7:3) mixture. Spectrum 5 refers to the solution of a mixture of double-labeled peptide DT2 and nonlabeled peptide DT0 in a 1:10 ratio in a chloroform−toluene (7:3) mixture. The results indicate that the dipole−dipole interaction between spin labels manifests itself only for peptide DT2 in chloroform−toluene (spectrum 4). Indeed, in this case, the spectrum is noticeably broadened as compared to the spectra of peptides DT1 and DT2 in MeOH and peptide DT1 in chloroform−toluene. Addition of the nonlabeled peptide DT0 leads to the narrowing of the peptide DT2 spectrum in chloroform−toluene (spectrum 5). A similar behavior was observed for the double-labeled analogues of trichogin GA IV

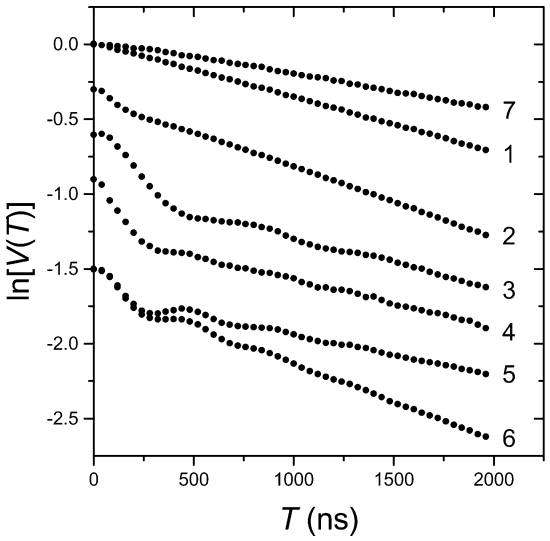

Figure 2. PELDOR signal decay $V(T)$ for the peptides studied in glassy solutions at 77 K: (1) DT1 in MeOH; (2) DT2 in MeOH; (3) DT1 in the chloroform−toluene (7:3) mixture; (4) DT2 in the chloroform−toluene (7:3) mixture; (5 and 6) DT2/DT0(1:10) in the chloroform−toluene (7:3) mixture at a total peptide concentration of 10^{-2} and 2×10^{-2} M, respectively; (7) difference between curve 6 and curve 5.

in the same chloroform−toluene mixture and was assigned to the occurrence of intramolecular dipolar interaction of spin labeled peptides that are clustered into peptide aggregates.[3]

The distinct broadening of CW-ESR spectrum lines in the case of DT2 solution in chloroform−toluene at 77 K (Figure 1, curve4) as compared with other ESR spectra (curves 1−3 and 5) is the result of strong dipolar coupling in this aggregate. We can assume that at least a part of the spin-lable pairs occur at the distances less than 1.0−1.2 nm. In this case, our variant of the PELDOR technique cannot be applied correctly. Having this in mind, we did not analyze the distance distribution effects for this specimes.

PELDOR Data. The PELDOR technique is more sensitive to weak dipole−dipole interactions than CW-ESR and makes it possible to study the interactions between spin labels hidden under the inhomogeneous ESR spectral broadening in the solid phase. Figure 2 illustrates the experimental PELDOR signal decay $V(T)$ for peptides DT1 and DT2 in frozen glassy solutions (for a convenient comparison, the curves in Figure 2 are shifted relative to each other along the vertical axis).

Curve 1 in Figure 2 belongs to the mono-labeled peptide DT1 in MeOH solution. In this case, we observe a simple exponential decay of $V(T)$ which is typical for a homogeneous random distribution of spin labels in the bulk. This curve suggests the absence of aggregation for these peptides in MeOH and parallels the previously reported observations for the mono-labeled analogues of trichogin GA IV in polar solvents.[3,4]

For the double-labeled peptide DT2 in MeOH solution (Figure 2, curve 2), a slightly faster decay of the signal is seen at short times T due to label coupling within the molecule. At longer times, the decay of $V(T)$, close to an exponential decay, is determined by the intermolecular interactions of the spin labels. A similar dependency has been already observed for the solutions of double labeled analogues of trichogin GA IV in polar solvents.[1−4]

Curves 3 and 4 in Figure 2 refer to the DT1 and DT2 peptides studied in the chloroform−toluene (7:3) mixture. Here we note a fast decay in the value of V at short times (at $T < 300-500$ ns) followed by a slow decrease in $V(T)$ accompanied by oscillations decaying with increasing T. A fast decay and oscillations of V with T definitely suggest peptide aggregation and are related to strong dipole−dipole interactions between spin labels in the aggregates.[3−5,17] In this case, the depth of the initial fast decay at short T depends on the probability to change the orientation of at least one spin in the aggregate by the pumping pulse. Therefore, this depth should increase with increasing number of spin labels in the aggregate. It is worthwhile to compare the depth of the initial fast decay for DT1 aggregates in chloroform−toluene (curve 3) with the initial decay for DT2 in methanol solution (curve 2). In the latter case, aggregation is absent, and therefore, interactions between only two nitroxides (those covalently linked to the same DT2 molecule) are in principle detectable. The depth of the initial fast decay is noticeably larger for curve 3 than for curve 2. The decay of the PELDOR signal observed for the nonaggregated double-labeled dimer is used to calibrate the number of spins involved in aggregates of mono-labeled molecules. This finding allows us to assume that in chloroform−toluene the number of peptide molecules per aggregate should exceed two.

The $V(T)$ decay at $T > 300-500$ ns strongly depends on the mean concentration of spin labels in solution. In this T region, the $V(T)$ decay is due to interaggregate dipole−dipole interactions for aggregated peptides in chloroform−toluene or to intramolecular interactions for peptides in methanol solution.[3−5,17] The concentration dependence of $V(T)$ is shown in Figure 2 (curves 5 and 6) for chloroform−toluene solutions of DT2/DT0 peptide mixtures (1:10). A similar acceleration of the relaxation decay due to the concentration growth of spin labels is found for DT1.

Intramolecular, Inter- and Intra-Aggregate Interactions between Spin Labels. The dependence of the PELDOR signal decay on peptide concentration is determined by the dipole−dipole interaction between spin labels belonging to different aggregates. Assuming that the dipole−dipole interactions between spin labels inside and between aggregates are independent of one another,[3−5] we can separate the contributions of these interactions to the general $V(T)$ decay. In this case, the $V(T)$ function can be represented as a product of the PELDOR signal decay due to the intra-aggregate interaction between spin labels, V_{INTRA}, and by the signal decay due to the interaggregate interaction between the spins V_{INTER}, i.e., $V = V_{INTRA}V_{INTER}$. As in previous paper,[1] we assume that the dependence of V_{INTER} on the concentration of spin labels C is of the exponential form $V_{INTER} = \exp[-p_b C f(T)]$, where p_b is the probability of spin flip induced by the pumping pulse and the function $f(T)$ determines the dependence of V_{INTER} on time T. From the experimental V_1 and V_2 decays derived for the concentrations of the spin-labeled peptide, C_1 and C_2, respectively, we can obtain the T dependencies for V_{INTER} and V_{INTRA} at a given concentration C_1 and C_2:

$$\ln(V_{INTER}) = C_1 \ln(V_2/V_1)/(C_2 - C_1) \quad (1)$$

$$\ln(V_{INTRA}) = \ln(V_1) - C_1 \ln(V_2/V_1)/(C_2 - C_1) = \ln(V_1) - \ln(V_{INTER}) \quad (2)$$

Similar relationships were used in to separate the inter- and intra-aggregate interactions between spin labels in the study of the spin-labeled analogous of trichogin GA IV.[1]

It is necessary to note that eqs 1 and 2 can be used for the determination of V_{INTRA} and V_{INTER} only if the intramolecular couplings do not change when the concentration of spin labels is changing. This means that the composition of the aggregates

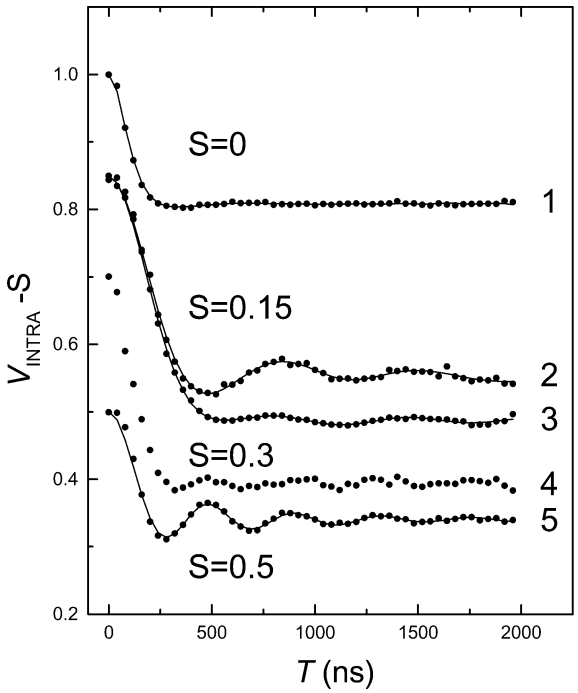

Figure 3. V_{INTRA} decay for the peptides studied: (1) DT2 in MeOH; (2 and 3) DT1 in the chloroform−toluene (7:3) mixture at peptide concentrations of 1.5×10^{-4} and 6×10^{-3} M, respectively; (4) DT2 in the chloroform−toluene (7:3) mixture; (5) DT2/DT0 (1:10) in the chloroform−toluene (7:3) mixture. Experimental values are represented as solid circles. The solid lines are calculated using the distribution functions $F(r)$ given in Figure 5. For convenience, the curves are shifted on S relative to 1. The S values are indicated.

should be steady or only slightly dependent on peptide concentration.

Curve 7 in Figure 2 shows the V_{INTER} decay for the DT2/DT0 mixture in chloroform−toluene obtained from curves 5 and 6 according to eq 1. The interaggregate contribution is a smooth curve without any oscillation, thus indicating that the intramolecular coupling between the two spin labels of DT2 in the aggregate practically do not change when the total concentration of peptide is doubled. Therefore, one can use relations 1 and 2 for determinating the V_{INTRA} decay.

As noted above for DT1 peptide aggregates in chloroform−toluene the intermolecular coupling within the aggregate is weakly dependent on the spin label concentration. This weak dependence can be the source of V_{INTER} distortion when using eqs 1 and 2 as the subtraction of intermolecular, intra-aggregate terms will not be complete. To reduce this effect the V_{INTRA} values were calculated from closely spaced concentrations (C_1 and C_2) values. Usually the ratio C_1/C_2 is selected as about 1.5. Using these particular V_{INTER} values, we determined from eqs 1 and 2 the contribution of intra-aggregate coupling at a given peptide concentration.

The solid circles in Figure 3 represent the V_{INTRA} decays obtained from relations 1 and 2 for the peptides studied. All dependencies have some oscillations (after a fast decay at short times) and they reach a limiting value for V_P. The final V_P values and the frequencies and depths of oscillations depend on both peptide structure and polarity of solvent. Solid lines shown in Figure 3 were calculated using the distance distribution function of the dipole dipole interaction between spin labels derived below. For convenience curves 2−5 were offset vertically by an amount S.

To compare with curves 2 and 3, curve 1 in Figure 3 was recorded for the nonaggregated peptide DT2 in MeOH solution. In this case, oscillations are very weak and only one-half-period with a small amplitude could be hardly observed. This finding indicates a wide distance distribution between spin labels in the peptide molecule.

Curves 2 and 3 in Figure 3 were obtained for aggregates of the mono-labeled DT1 in chloroform−toluene at peptide concentrations of 1.5×10^{-4} and 6×10^{-3} M, respectively. As the peptide concentration increases, both the oscillation depth and the V_P value decrease. This result is indicative of the existence of different aggregates and of the shift in equilibrium with increasing concentration toward aggregates with a larger number of spin-labeled molecules.[7] As compared to the spin-labeled analogues of trichogin GA IV,[7] where the equilibrium is almost completely shifted toward aggregates with four molecules at a peptide concentration of about 10^{-3} M, in this case, a complete shift is not attained. This makes the estimation of the number of peptide molecules in the aggregates from the relationships used in refs 3−5 and 17 not very reliable.

Curves 4 and 5 in Figure 3 were obtained for solutions of the double-labeled peptide DT2 and the DT2/DT0 mixture in chloroform−toluene, respectively. As mentioned above, the CW-ESR spectrum of peptide DT2 under these conditions is broadened as compared to the other spectra (Figure 1). In addition, the limiting value of V_P (Figure 3) is smaller than that observed for the DT2 solution in MeOH. These CW-ESR spectra and PELDOR data indicate the onset of aggregates of peptide DT2 in the chloroform−toluene mixture similarly to the peptide aggregates of DT1 in the same solvent mixture. The weak amplitude of the oscillations of the $V(T)$ decay point to the existence of some distance distribution between spin labels in the aggregates. Addition of a 10-fold excess of peptide DT0 to the peptide DT2 solution changes substantially both the CW-ESR spectrum and the $V(T)$ decay as compared with the solution of peptide DT2 alone. The width of the lines in the CW ESR spectrum becomes smaller (Figure 1). The narrowing of the spectrum lines is accompanied by a noticeable increase of the oscillation depth and a moderate increase of the V_P value (from 0.7 up to 0.8) as it follows from a comparison of curves 4 and 5 of Figure 3. These results suggest that aggregates of nonlabeled molecules (DT0) with a small fraction of double-labeled molecules (DT2) are formed. Indeed, the addition of nonlabeled peptide has no effect on the oscillation frequency. In this case, the intramolecular dipole−dipole interaction between the two labels of DT2, present in the aggregate of nonlabeled molecules, is of major importance.

Distance Distribution between Spin Labels: PELDOR Calculations. The PELDOR signal decay $V(T)$ is determined by the dipole−dipole interaction between unpaired electrons. The dipole−dipole interaction between labels depends on both the distance between labels, r, and the orientation of external magnetic field, **B**, relative to a vector connecting spin labels, $\boldsymbol{r}$ (see Figure 4, a). This makes it possible to study the peculiarities of the mutual 3D distribution of spin labels by the PELDOR technique.

The spin-labeled peptides under study in frozen glassy solutions are randomly space-oriented. The shape of the ESR spectra of the randomly oriented nitroxyl spin labels in a solid phase is mainly determined by anisotropy of both the hyperfine interaction of an unpaired electron with a nitrogen nucleus and a g factor, i.e., the parameters of $\boldsymbol{A}$ and $\boldsymbol{g}$ tensors, respectively. This leads to the orientational selectivity in the ESR spectra; that is, each spectrum point corresponds to a set of spatial

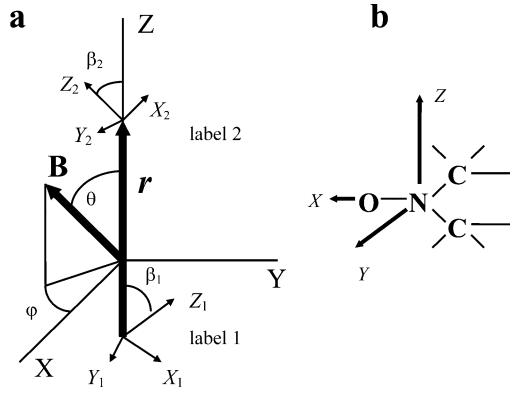

Figure 4. Orientation of the spin label axes in molecular frame (a) and the structure of the nitroxyl fragment (b).

orientations of spin labels, for which resonance occurs at a given point of the spectrum.

For PELDOR of the nitroxyl spin labels, the pulses forming a spin−echo signal and a pumping pulse have effect only on a small part of ESR spectrum. The pulses located at certain points of the ESR spectrum excite only the orientations of nitroxyl fragments that correspond to pulse positions in the spectrum. The resulting selectivity in nitroxyl fragment orientations relative to the external magnetic field can cause selectivity in the orientation of the vector ***r***, which should be taken into account in the analysis of experimental data.[19]

One of the aims of the present work was to obtain the functions of distance distribution between spin labels. To this end, the experimental dependencies $V(T)$ were compared with the calculated dependencies for specified experimental conditions with respect to the orientational selectivity. The calculations were based on the PELDOR signal decay law for the pairs of spin labels with a fixed distance r between labels in a pair and a fixed angle θ between **B** and vector ***r*** with subsequent averaging over angle θ.[17] It is worth noting that, in the general form, the problem of finding the distance distribution functions in the absence of orientational selectivity was solved Jeschke et al.[20]

For the similarly oriented pairs of spin labels with a fixed angle θ between **B** and the vector ***r*** connecting spin labels 1 and 2 in a pair, the position of resonance frequencies ν_1 and ν_2 for spin labels in a pair will depend on the spatial orientation of spin labels. In this case, the PELDOR signal decay, V_θ, can be given as[17]

$$V_\theta = \left\langle\left\langle V_{1,2}\left(1 - p_{1,2}\left(1 - \cos\left[\frac{\gamma^2\hbar T}{r^3}(1 - 3\cos^2\theta)\right]\right)\right)\right\rangle_1\right\rangle_2 = V_\theta(0)\left(1 - p_b(\theta)\left(1 - \cos\left[\frac{\gamma^2\hbar T}{r^3}(1 - 3\cos^2\theta)\right]\right)\right) \quad (3)$$

where

$$V_\theta(0) = \langle\langle V_{1,2}\rangle_1\rangle_2;\ p_b(\theta) = \frac{\langle\langle V_{1,2}p_{1,2}\rangle_1\rangle_2}{\langle\langle V_{1,2}\rangle_1\rangle_2} \quad (4)$$

The $V_{1,2}$ values in eqs 3 and 4 are the spin−echo signal at frequency ν_A from the spin label pairs with a given frequencies ν_1 and ν_2; $p_{1,2}$ is the probability of spins B rotation in the same pairs; r is the distance between spin labels in a pair; $\langle..\rangle_1$ and $\langle..\rangle_2$ denote the averaging over frequencies ν_1 and ν_2, respectively. For the given frequencies ν_1 and ν_2, the values of $V_{1,2}$ and $p_{1,2}$ were calculated from the relationships[21]

$$V_{1,2} = \sum_{k=1}^{2}\frac{1}{\Omega_{A,k}^3}\sin[\phi_{1A}\Omega_{A,k}]\sin^2\left[\frac{1}{2}\phi_{2A}\Omega_{A,k}\right] \quad (5)$$

$$p_{1,2} = \sum_{k=1}^{2}\frac{1}{\Omega_{B,k}^2}\sin^2\left[\frac{1}{2}\phi_B\Omega_{B,k}\right] \quad (6)$$

$$\Omega_{A,k} = \left(1 + \left(\frac{\nu_k - \nu_A}{\nu_{1A}}\right)^2\right)^{1/2};\ \Omega_{B,k} = \left(1 + \left(\frac{\nu_k - \nu_B}{\nu_{1B}}\right)^2\right)^{1/2} \quad (7)$$

where $k = 1$ and 2 is a number of the spin label in the pair; ν_A and ν_B are the frequencies of the pulses forming echo and the pumping pulse, respectively; ϕ_{1A} and ϕ_{2A} are the rotation angles of resonance spins A under the action of the first and second pulses, respectively; ϕ_B is the rotation angle of resonance spins B under the action of the pumping pulse; ν_{1A} and ν_{1B} denote the amplitudes of mw pulses and the pumping pulse, respectively, given in frequency units. Later on, we used the experimental values of the above parameters.

To obtain the PELDOR signal from the randomly oriented pairs of spin labels for a given distance r between the labels, eq 3 should be averaged over the angle θ

$$V_r = \langle V_\theta\rangle_\theta = V_r(0)\left(1 - p_b\left(1 - \frac{\left\langle V_\theta(0)p_b(\theta)\cos\left[\frac{\gamma^2\hbar T}{r^3}(1 - 3\cos^2\theta)\right]\right\rangle_\theta}{\langle V_\theta(0)p_b(\theta)\rangle_\theta}\right)\right) \quad (8)$$

where

$$V_r(0) = \langle V_\theta(0)\rangle_\theta;\ p_b = \frac{\langle V_\theta(0)p_b(\theta)\rangle_\theta}{\langle V_\theta(0)\rangle_\theta} \quad (9)$$

and $\langle...\rangle_\theta$ denotes the averaging over the angle θ.

In the presence of the distance distribution between the labels, eq 8 should be averaged with a corresponding distance distribution function $F(r)$. Take into account that the product $F(r)\,dr$ is a fraction of spin label pairs in the distance range of r to $r + dr$, the expression for the PELDOR signal decay normalized to the signal at $T = 0$ is of the form

$$V = 1 - p_b + p_b\int_0^\infty F(r)U(r,T)\,dr \quad (10)$$

where

$$U(r,T) = \frac{\left\langle V_\theta(0)p_b(\theta)\cos\left[\frac{\gamma^2\hbar T}{r^3}(1 - 3\cos^2\theta)\right]\right\rangle_\theta}{\langle V_\theta(0)p_b(\theta)\rangle_\theta} \quad (11)$$

As T increases, the function $U(r,T)$ tends to zero and the value of V in eq 7 reaches its limiting value $V_p = (1 - p_b)$.

Equations 10 and 11 refer to the case of spin label distribution in the form of randomly oriented pairs. To a first approximation, they can be also used to describe PELDOR signal decay for the groups of spin labels containing more than two labels. This approach holds for the case where the number of spin labels in a group is not too great and the probability of excitation of more than two spins by MW pulses can be neglected. Relation 10, in

this case, will be valid if $1 - V_P = p_b(N - 1) \ll 1$where N is the number of labels in the group.[17] In our experiments, for the aggregates of mono-labeled peptides, the value of $1 - V_P$ was about 0.36 (see Figure 3) and the condition $(1 - V_P) \ll 1$ can be considered satisfied. Taking this condition into account, relations 10 and 11 were used for describing the aggregates of mono-labeled peptides.

As mentioned above, for a fixed angle θ, the frequencies ν_k and ν_j included in eqs 3−7 depend on the principal values of tensors $\boldsymbol{A}$ and $\boldsymbol{g}$ and its orientation in the molecular frame. For the nitroxyl fragment, the principal axes of $\boldsymbol{A}$ and $\boldsymbol{g}$ tensors coincide. In this case, the x axis is directed along the N−O bond, the z axis runs along the $2p\pi$ orbital of the unpaired electron, and the y axis is perpendicular to the xz plane. If according to Parmon et. al,[22] we employ a radical pair molecular coordinate system, in which the Z axis is directed along the vector $\boldsymbol{r}$ connecting spin labels, then the frequencies ν_k and ν_j depend both on six Euler angles giving the orientation for the axes of radical fragments in a molecular coordinate system and on the angle φ between the X axis of a molecular coordinate system and the magnetic field projection onto the XY plane.[22] Figure 4 shows schematically the orientation of the principal axes in the molecular frame and the structure of the nitroxyl fragment. Because the angle φ is not included in the relationship for calculating the PELDOR signal, all calculations were performed for the random orientation of the magnetic field **B** over the angle φ. In addition to the anisotropy of $\boldsymbol{A}$ and $\boldsymbol{g}$ tensors, we took into account the supplementary broadening of the ESR spectrum due to the interaction between the unpaired electrons and the surrounding magnetic nuclei.

Knowing the $U(r,T)$ function, we can obtain the distance distribution function $F(r)$ between the labels from experimental data using eqs 10 and 11. A particular form for $U(r,T)$ for the given orientations of nitroxyl fragments at a fixed distance r and a random value of angle φ was calculated numerically from the experimental parameters for the microwave pulses and ESR spectrum. In the calculations, we used the following main values for $\boldsymbol{A}$ and $\boldsymbol{g}$ tensors: $A_{xx} = 4.0$ G, $A_{yy} = 7.0$ G, and $A_{zz} = 35.0$ G; $g_{xx} = 2.0095$, $g_{yy} = 2.0061$, and $g_{zz} = 2.0025$. The line shape determined by the other sources of broadening was considered Gaussian with a width between the points of the maximum slope of 3.9 G. The ESR spectra calculated using these parameters coincide well with the experimental TOAC spectra in the systems studied. The experimental parameters contained in eqs 5−7 were as follows: $\nu_A = 9.476$ GHz, $\nu_A - \nu_B = 65$ MHz, $\nu_{1A} = 6.2$ MHz, $\nu_{1B} = 12.5$ MHz, $\phi_{1A} = 90°$, $\phi_{2A} = 180°$, and $\phi_B = 180°$. The position of lines in the spectrum for the given orientations of a pair and nitroxyl fragments in a pair was calculated using eqs 1−6 from ref 22 in the absence of exchange and dipole interaction between spin labels.[22]

The results from the preliminary analysis indicate that the $U(r,T)$ function form depends at a given r on the angles β_1 and β_2 between the Z axis of a molecular coordinate system and the z axes of the first and second radical fragments, respectively. The dependence on the orientation of the x and y axes of radical fragments appeared to be weak and was neglected. Thus, $U(r,T)$ was calculated for the different values of the β_1 and β_2 angles for the other Euler angles[22] equal to zero. In some cases, calculations were also performed for the random orientation of radical fragments in radical pair.

Distance Distribution between Space Labels. Comparison with Experiment. The $F(r)$ function was derived using numerical calculations of the PELDOR signal decay $V(T)$ from eqs 3−11. To this end, the distance range of 1 nm $\leq r \leq$ 7 nm was divided into intervals with the step $\delta r = 0.1$ nm. From eq 11, we calculated the values of $U(r_k, T_m)$ for each point r_k, where the T_m values correspond to the experimental values of time T for the points at which the PELDOR signal amplitude was measured. The $U(r_k,T)$ functions were calculated at the fixed values of the angles β_1 and β_2. Substituting integral in eq 10 by the sum, the value of V at each point T_m was of the form

$$V_m = V_P + (1 - V_P)\sum_k F(r_k)U(r_k,T_m)\delta r \qquad (12)$$

By varying the values of $F(r_k)$, we determined the set of $F(r_k) \geq 0$ at which the sum of the squares of the differences, Δ, between the experimental and calculated PELDOR signals was minimal

$$\Delta = \sum_m (V(T_m) - V_m)^2 = \min \qquad (13)$$

where $V(T_m)$ are the experimental values of the PELDOR signal measured at the points T_m, and V_m are the values of the PELDOR signal calculated from eq 12 using the experimental values of V_P. In this case, the Δ value depends on 61 variables $F(r_k)\delta r$ lying in the range from 0 to 1. $F(r_k)\delta r$ values corresponding to minimal Δ have been found by calculations started from the accidential $F(r_k)\delta r$ values and moving along the Δ gradient to the minimal Δ values. Provisional calculation of the $U(r_k,T_m)$ function allows us to hasten the numerical calculations and make the distance distribution function averaging over starting $F(r_k)\delta r$ values. The calculation of single $F(r)$ by this method takes about 1 h by using not very fast PS.

The $F(r)$ functions were calculated by the above method for each experimental $V(T)$ decay by varying the values of the angles β_1 and β_2. From the solutions obtained, we have chosen those for which the Δ value was minimal, i.e., giving the best coincidence between the experimental and calculated dependencies of the PELDOR signal decays $V(T)$. It is established that the minimum value of Δ can be reached in some range of the angles β_1 and β_2. Because within this range the form of the $U(r,T)$ function depends on the particular values of the angles β_1 and β_2, we get from eqs 12 and 13 the set of distribution functions $F(r)$ that satisfy the experimental data. This allows us to estimate the ambiguity of the $F(r)$ form caused by the calculation approach employed in the present work. To this end, the figures below show the distribution functions for the edges and the center of the range of the angles β_1 and β_2 used. Note, that calculated $F(r)$ functions appeared the same for angles β and $\pi-\beta$; therefore, we shall show data for $\beta_1,\beta_2 \leq \pi/2$ angles. Our calculations show that the possible boundary values for β_1 and β_2 angles which correspond to the minimum of Δ values make the limits in spin labels orientation around Z in peptides studied.

Figure 5 shows the distance distribution functions $F(r)$ obtained for a series of experimental V_{INTRA} decays represented by the solid circles in Figure 3. The solid lines in Figure 3 were calculated from eq 12 using the distribution functions shown in Figure 5. The oscillations decay for PELDOR signals calculated using these $F(r)$ is in good agreement with the experimental one (Figure 3).

Curve 1 in Figure 5 is obtained from experimental dependence 1 in Figure 3 and refers to the DT2 in MeOH solution. In this case, the minimum of the Δ value is almost independent of the values of the β_1 and β_2 angles over the entire range of 0 to $\pi/2$ and is close to the value of the random orientation of nitroxyl labels in a pair. The open circles in curve 1 were obtained for

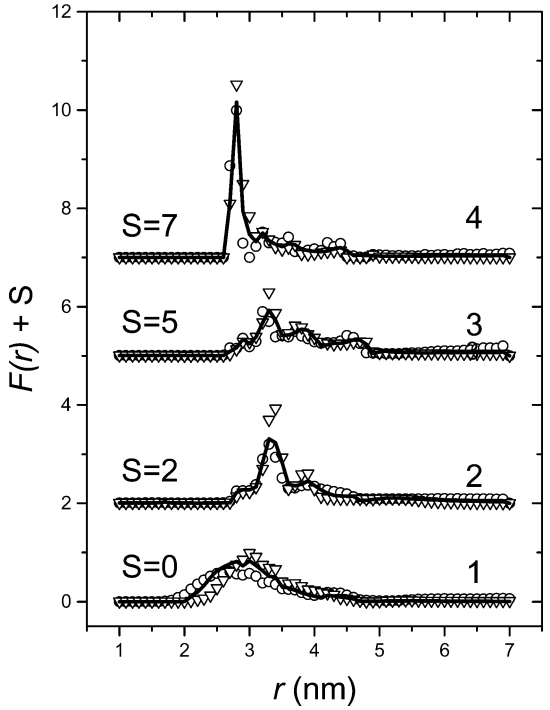

Figure 5. Distance distribution functions between spin labels in frozen solutions at 77 K: (1) DT2 in methanol, circles are obtained at $\beta_1 = \beta_2 = 0$, triangles are obtained at $\beta_1 = \beta_2 = \pi/2$, solid line was obtained for random orientation of spin labels; (2 and 3) DT1 in chloroform/toluene (7:3) at peptide concentrations of 1.5×10^{-4} and 6×10^{-3} M, respectively: circles are obtained at $\beta_1 = \beta_2 = 0$, triangles are obtained at $\beta_1 = \beta_2 = 40°$, solid lines are obtained for $\beta_1 = 0$, $\beta_2 = 40°$; (4) DT2 +DT0 (1:10) in chloroform/toluene (7:3): circles are obtained at $\beta_1 = \beta_2 = 0$, triangles are obtained at $\beta_1 = \beta_2 = 30°$, solid lines are obtained for $\beta_1 = 0$ and $\beta_2 = 30°$.

$\beta_1 = \beta_2 = 0$ and the triangles were obtained for $\beta_1 = \beta_2 = \pi/2$. The solid line denotes the random orientation of radical fragments. The solid line in Figure 3 curve 1 shows $V(T)$ calculated for the random orientation of spin labels in molecule. The $V(T)$ dependencies calculated for $\beta_1 = \beta_2 = 0$ and $\beta_1 = \beta_2 = \pi/2$ coincide with that denoted by the solid line. As follows from Figure 5, the distribution function $F(r)$ for peptide DT2 in MeOH is a wide asymmetric curve. The mean distances between the labels $\langle r \rangle$ and the mean square of distance $\langle r^2 \rangle$ obtained using the solid line in curve 1 are 3.1 and 10.0 nm^2, respectively The most probable value of the distances corresponding to the $F(r)$ maximum is 2.9 nm.

Curves 2 and 3 in Figure 5 were obtained from dependencies 2 and 3 in Figure 3, respectively. These curves refer to the aggregates of the mono-labeled peptide DT1 in the frozen glassy chloroform−toluene mixtures. The concentrations of peptide molecules in solutions were 1.5×10^{-4} and 6×10^{-3} M, respectively. The Δ value for both of the curves is minimal over the range of the angles β_1 and β_2 from 0 to 40°. The open circles in curves 2 and 3 were obtained for $\beta_1 = \beta_2 = 0$ and the triangles were obtained for $\beta_1 = \beta_2 = 40°$. The solid line refers to the intermediate case of $\beta_1 = 40°$ and $\beta_2 = 0$. The solid lines in curves 2 and 3 in Figure 3 were calculated for the distribution functions denoted by solid lines in curves 2 and 3 in Figure 5. The $V(T)$ decays calculated for $\beta_1 = \beta_2 = 0$ and 40° almost fully coincide with the above curves and are, therefore, omitted in Figure 3. The distance distribution functions for curve 2 in Figure 5 extend from 3.0 to 4.5 nm. The maximum is observed at a distance of 3.3 nm. On transition to curve 3 in Figure 5, we observed a noticeable broadening in the distribution function and a relative decrease in a maximum for $r = 3.3$ nm.

Curve 4 in Figure 5 refers to the peptide DT2 molecules isolated in the aggregates of nonlabeled peptide molecules in a chloroform−toluene (7:3) mixture. Curve 4 was obtained from experimental dependence 5 in Figure 3. The minimum values of Δ for this case are observed over a relatively narrow range of the angles β_1 and β_2 of 0°−30°. As in the previous cases, curve 4 in Figure 5 shows the distribution functions for the edges and the center of the range of the angles β_1 and β_2. The open circles in curves 2 and 3 were obtained for $\beta_1 = \beta_2 = 0$ and the triangles were obtained for $\beta_1 = \beta_2 = 30°$. The solid line refers to the intermediate case of $\beta_1 = 30°$ and $\beta_2 = 0$. These $F(r)$ functions were used for calculating the $V(T)$ decay. The solid line in curve 5 in Figure 3 was calculated using distribution function shown by the solid line for dependence 4 in Figure 5. The $V(T)$ dependencies calculated for $\beta_1 = \beta_2 = 0$ and 30° almost fully coincide with the above curve. Therefore, these are omitted in Figure. 3. In this case, the distance distribution function is a single line with a maximum at 2.8 nm and a half-width at a half-height of about 0.1 nm. The oscillation frequency of experimental curve 5 in Figure 3 coincides with the position of the distribution function maximum.

The distance distribution functions between spin labels for the double-labeled peptide DT2 demonstrate a substantial solvent effect on the peptide structure. A wide distance distribution between spin labels is observed for the DT2 peptide in MeOH solution. The ratio between the mean-square deviation and the mean distance $(\langle r^2 \rangle - \langle r \rangle^2)^{1/2}/\langle r \rangle$ is about 0.2, which indicates the existence of a wide set of conformations for the molecules of a given peptide in methanol. The existence of a wide set of conformations causes, in this case, the absence of dependence on the orientation of radical fragments. The distance distribution function for the labels of DT2 isolated within the aggregates of unlabeled peptides is a narrow line with a maximum at a distance of 2.8 nm and a half-width at a half-height of 0.1 nm. A distance of 2.8 nm between spin labels corresponds to the structure of the α-helix type for the peptide molecule shown in Figure 6. The range of the orientations of the z axes of radical fragments of 0−30° is also in fair agreement with the structures in Figure 6.

A comparison between the distance distribution functions for the aggregates of peptide DT1 in the chloroform−toluene mixture at different peptide concentrations (curves 2 and 3 in Figure 5) shows that an increase in concentration causes a relative decrease in a maximum at 3.3 nm. Thus, this maximum is assumed to correspond to the distance between labels in the aggregate of two peptide DT1 molecules. As the peptide concentration in solution increases, the equilibrium shifts toward the formation of aggregates with a larger number of molecules, which causes a decrease of the fraction of aggregates of two molecules and a corresponding decrease in the relative value of the maximum. It is reasonable to assume that a distance of 3.3 nm also exists in the aggregates with a larger number of peptide molecules if these aggregates include those of two molecules as structural units. To obtain this distance between the labels in the aggregate of two DT1 molecules, it is necessary that the molecules in this aggregate would be in antiparallel disposition. Similar conclusions have been drawn for the aggregates of shorter spin-labeled analogues of trichogin GA IV in the same solvent by estimating distances between labels from the period of PELDOR signal oscillations.[3,6]

Secondary Structure of the Covalently Bound Dimer. The distance between two TOAC residues located on the same peptide molecule is related to the average secondary structure adopted by the peptide chain.[5] It should be remembered that

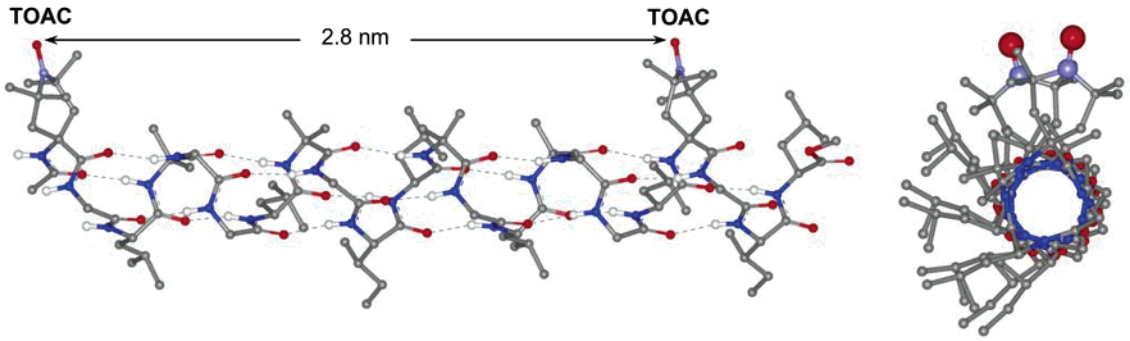

Figure 6. α-Helical model for DT2 shown in two perpendicular orientations.

because of the high content of helix-promoting Aib residues, peptaibols tend to fold into helical structures of the α/3_{10}-type. Therefore, the intramolecular TOAC/TOAC separation in doubly labeled peptide molecules depends heavily not only on the ordered/disordered but also on the type of the ordered (helical) conformation adopted by the peptide. A circular dichroism (CD) study (spectra not shown) performed on our trichogin dimers points to the conclusion that a large amount of ordered, helical structures are present in methanol solution at room temperature. Our PELDOR data, obtained in the same solvent used for the CD measurements but at 77 K, indicate that besides helical structures other conformations are present in the equilibrium mixtures. Indeed, disordered conformations, most likely located at the N- and C-termini of the peptide chains, may equilibrate with helical structures. The other possible reason for observed disorder could be the strain created by formation of glassy matrix cooling the methanol at 77 K. This result invites further investigations.

In weak polar solvents, the distance between the two TOAC residues in DT2 (2.8 nm) matches well with the distance (2.7 nm) calculated from an α-helical molecular model (Figure 6). It should be remembered, however, that the conformation of trichogin GA IV in chloroform−toluene appears to be largely 3_{10} helical.[2,5] Thus, it appears that the conformations of trichogin dimers and monomers are different. This result is consistent with the finding by Karle and Balaram,[23] based on a statistical analysis of X-ray structures, according to which the α helix is favored over the 3_{10} by longer peptide chains and/or smaller percentages of Aib residues. The thermodynamics of the coil-to-helix transition may also help in understanding the type of secondary structure adopted by a particular peptide chain.[24]

Tertiary Structure of the Aggregate. Our PELDOR results indicate that the intermolecular distance between the spin labels in the aggregate of mono-labeled dimer molecules in chloroform−toluene is about 3.3 nm. A comparison between the distance distribution functions for the aggregates of peptide DT1 in the chloroform−toluene mixture at different peptide concentrations (curves 2 and 3 in Figure 5) shows that an increase in concentration causes a relative decrease in the maximum at 3.3 nm. Thus, this maximum is assumed to correspond to the distance between labels in the aggregate of two DT1 molecules. As the peptide concentration in solution increases, the equilibrium shifts toward the formation of aggregates with a larger number of molecules, which causes a decrease of the fraction of aggregates of two molecules and a corresponding decrease in the relative value of the maximum. It is reasonable to assume that a distance of 3.3 nm also exists in the aggregates with a larger number of peptide molecules, provided these aggregates include those with two molecules as the structural units.

The observed intermolecular distance separating the nitroxides of DT1 molecules would correspond to an antiparallel, face-to-face orientation of two molecules (Figure 7A). The helix dipole moment has also to be taken into account. Indeed, it is generally believed that such a molecular dipole moment is an important parameter for a proper understanding of the spatial organization of helical domains in proteins and amphipathic molecules in self-assembled peptide clusters.[25−28] The dipole of each peptide bond is 3.5 D (0.72 eÅ; 1.1×10^{-29} Cm) and is approximately oriented parallel to the N−H and O═C bonds. Therefore, when DT1 folds into an α-helical structure, its total dipole moment results to be 77.0 D and oriented parallel to the helix axis. Thus, by combining this information with the experimental TOAC/TOAC distance (3.3 nm) revealed be the PELDOR analysis, we suggest that in the chloroform/toluene mixture two DT1 molecules aggregate with antiparallell orientation (Figure 7A). In addition, as the aggregates are energetically favored when the dipoles are located at the shortest possible distance, we propose as a reasonable model the dimer illustrated in panels B and C of Figure 7, in which the least sterically hindered (and also least hydrophobic) Gly residues of the two molecules are facing each other. In this model, the distance

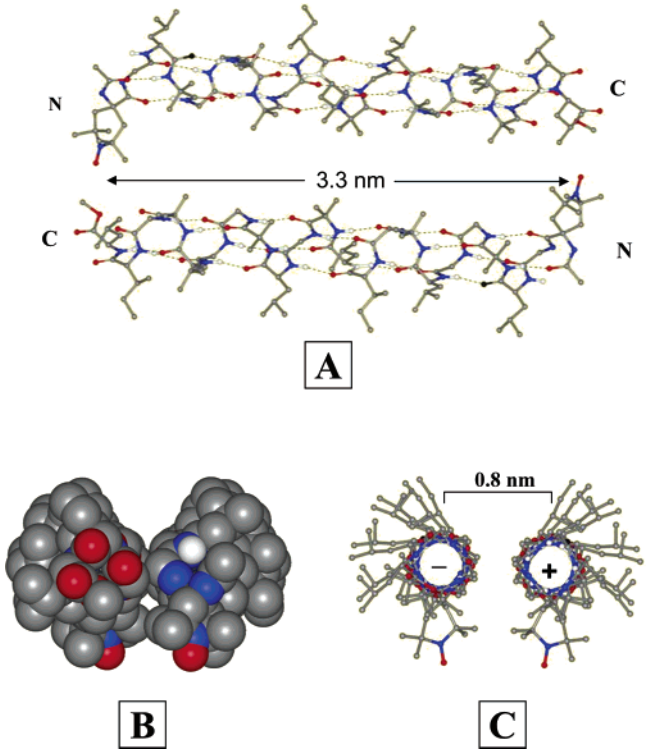

Figure 7. Proposed model for antiparallel, two-helices aggregation by DT1. (A) side-view; (B) space-filling; and (C) stick and ball, view along the helix axis with the two peptide molecules of the aggregate positioned at the shortest possible distance.

(from axis to axis) separating the two helical molecules ends up being about 0.8 nm.

Some differences appear when the aggregates formed by trichogin[3,6] and trichogin dimers (this work) are compared. Trichogin GA IV forms mainly tetrameric assemblies of molecules with prevailing 3_{10}-helical conformations, whereas the trichogin dimers DT1 and DT2 seem to prefer α-helical structures. However, the tertiary structures of the aggregates of trichogin GA IV and its covalent dimers appear to share the antiparallell orientation of the helical molecules, the polar sides of which face the center of the aggregate cluster.

Conclusions

In this work, the method of pulsed electron−electron double-resonance in electron spin−echo (PELDOR) was used to study the dipole−dipole interaction between spin labels for frozen glassy solutions of spin-labeled analogous of the head-to-tail dimer of trichogin GA IV. In the apolar chloroform−toluene (7:3) mixture, the dimer (two head-to-tail, covalently linked trichogin GA IV molecules) forms aggregates the composition of which depends on peptide concentration. No aggregation was detected in MeOH solution.

The PELDOR signal decay kinetics due to intramolecular coupling of spin labels in the molecules of the double-labeled covalent dimer were analyzed. Distance distribution functions for the spin labels internal to the peptides and in the aggregates were calculated. We observed for the double-labeled dimer DT2 in MeOH solution, where no aggregates are formed, a wide distance distribution between the two intramolecularly positioned labels with an average value of 3.1 nm. In weakly polar solvents, where aggregates are observed for DT2, the distribution function displays a sharp maximum at 2.8 nm with a half-width at half-height of about 0.1 nm. It is worth noting that a distance between the labels of 2.8 nm is fully compatible with the adoption by DT2 of an α-helical structure.

The PELDOR signal decay kinetics due to the couplings of spin labels in the aggregates of the mono-labeled peptide in the chloroform−toluene mixture were extracted from the general PELDOR decay. An increase in peptide concentration from 1.5×10^{-4} to 6×10^{-3} M induces a shift toward formation of aggregates with a larger number of molecules. The distance distribution function between spin labels was obtained. We demonstrated that this shift leads to a decrease in the population of the spin label pairs separated by 3.3 nm.

For the aggregate of the covalently bound, trichogin dimer, a face-to-face aligned model of molecules with antiparallel orientation is proposed.

Acknowledgment. The authors are grateful to Dr. G. Jeschke for providing them with the preprint of his recent article.[20] This work was supported by The Netherlands Organization of Scientific Research (NWO), Project 047.009.018, and by the Russian Foundation of the Basic Research (RFBR), Grants 00-15-97321, 02-03-32022, 00-03-40124, NWO-RFBR Grant 030389011, INTAS Grant 00-04-04.

Supporting Information Available: The synthesis, purification and characterization head-to-tail dimers of TOAC spin-labeled trichogin GA IV described in details. This material is available free of charge via the Internet at http://pubs.acs.org.

References and Notes

(1) Milov, A. D.; Maryasov, A. G.; Tsvetkov, Yu. D.; Raap, J. *Chem. Phys. Lett*. **1999**, *303*, 135−143.
(2) Milov, A. D.; Maryasov, A. G.; Samoilova, R. I.; Tsvetkov, Yu. D.; Raap, J.; Monaco, V.; Formaggio, F.; Crisma, M.; Toniolo, C. *Dokl. Acad. Nauk* **2000**, *370*, 265−268.
(3) Milov, A. D.; Tsvetkov, Yu. D.; Formaggio, F.; Crisma, M.; Toniolo, C.; Raap, J. *J. Am. Chem. Soc.* **2000**, *122*, 3843−3848.
(4) Milov, A. D.; Tsvetkov, Yu. D.; Raap, J. *Appl. Magn. Reson.* **2000**, *19*, 215−227.
(5) Milov, A. D.; Tsvetkov, Yu. D.; Formaggio, F.; Crisma, M.; Toniolo, C.; Raap, J. *J. Am. Chem. Soc.* **2001**, *123*, 3784−3789.
(6) Milov, A. D.; Tsvetkov, Yu. D.; Formaggio, F.; Crisma, M.; Toniolo, C.; Millhauser, G. L.; Raap, J. *J. Phys. Chem. B* **2001**, *105*, 11206−11213.
(7) Milov, A. D.; Tsvetkov, Yu. D.; Formaggio, F.; Crisma, M.; Toniolo, C.; Raap, J. *Advanced EPR Applied to Biosciences, Satellite Symposium B in APES′01*, November 1−3, 2001; Kawamori, A., Ed.; pp 99−108.
(8) Milov, A. D.; Tsvetkov, Yu. D.; Gorbunova, E. Yu.; Mustaeva, L. G.; Ovchinnikova, T. V.; Raap, J. *Biopolymers* **2002**, *64*, 328−336.
(9) Toniolo C.; Crisma M.; Formaggio F.; Peggion C.; Epand R. F.; Epand R. M. *CMLS, Cell. Mol. Life Sci.* **2001**, *58*, 1179−1188.
(10) Kropacheva, T. N.; Raap, J. *Biochim. Biophys. A* **2002**, *1567*, 193−203.
(11) Bechinger, B.; Skladnev, D. A.; Ogrel, A.; Li, X.; Rogozhkina, E. V.; Ovchinnikova, T. V.; O'Neil, J. D. J.; Raap, J. *Biochemistry* **2001**, *40*, 9428−9437.
(12) Monaco, V.; Formaggio, F.; Crisma, M.; Toniolo, C.; Hanson, P.; Millhauser, G. *Biopolymers* **1999**, *50*, 239−253.
(13) Toniolo, C.; Peggion, C.; Crisma, M.; Formaggio, F.; Shui, X.; Eggleston, D. S. *Nature Struct. Biol.* **1994**, *1*, 908−914.
(14) Monaco, V.; Formaggio, F.; Crisma, M.; Toniolo, C.; Hanson, P.; Millhauser, G.; George, C.; Deschamps, J. R.; Flippen-Anderson, J. L. *Bioorg. Med. Chem.* **1999**, *7*, 119−131.
(15) Rassat, A.; Rey, P. *Bull. Chem. Soc. Fr.* **1967**, 815−817.
(16) Toniolo, C.; Crisma, M.; Formaggio, F. *Biopolym. (Pept. Sci.)* **1998**, *47*, 153−158.
(17) Milov, A. D.; Maryasov, A. G.; Tsvetkov, Yu. D. *Appl. Magn. Reson.* **1998**, *15*, 107−143.
(18) Carpino, L. A. *J. Am. Chem. Soc.* **1993**, *115*, 4397.
(19) Larsen, R. G.; Singel, D. J. *J. Chem. Phys.* **1993**, *98* (7), 5134−5146.
(20) Jeschke, G.; Koch, A.; Jonas, U.; Godt, A. *J. Magn. Reson.* **2002**, *155*, 72−82.
(21) Salikhov, K. M.; Semenov, A. G.; Tsvetkov, Yu. D. *Electron Spin−Echo and its Applications*; Novosibirsk: Nauka, 1976; in Russian.
(22) Parmon, V. N.; Kokorin, A. I.; Zhidomirov, G. M. *J. Magn. Reson.* **1977**, *28*, 339−349.
(23) Karle, I. L.; Balaram, P. *Biochemistry* **1990**, *29*, 6747−6756.
(24) Millhauser, G. L. *Biochemistry* **1995**, *34*, 3873−3877.
(25) Wada, A. *Adv. Biophys.* **1976**, *9*, 1−63.
(26) Hol, W. G.; von Duijen, P. T.; Berendsen, H. J. C. *Nature* **1978**, *273*, 443−446.
(27) Hol, W. G. L. *Adv. Biophys.* **1985**, *19*, 133−165.
(28) Hol, W. G. L.; Halie, L. M.; Sander, C. *Nature* **1981**, *294*, 532−536.